COMPUTER METHODS IN MATERIALS SCIENCE

2021, vol. 21, no. 2, 95–104
https://doi.org/10.7494/cmms.2021.2.0739

A new BEM for modeling and simulation of 3T MDD laser-generated ultrasound stress waves in FGA smart materials

Mohamed A. Fahmy[1,2]

[1] Jamoum University College, Umm Al-Qura University, Alshohdaa 25371, Jamoum, Makkah, Saudi Arabia.
[2] Faculty of Computers and Informatics, Suez Canal University, New Campus, 4.5 Km, Ring Road, El Salam District, 41522 Ismailia, Egypt.

Abstract

The goal of this study is to present a new theory known as the three-temperature memory-dependent derivative (MDD) of ultrasound stress waves in functionally graded anisotropic (FGA) smart materials. It is extremely difficult to address the difficulties related to this theory analytically due to its severe nonlinearity. As a result, we suggest a new boundary element method (BEM) to solve such equations. The suggested BEM technique incorporates the benefits of both continuous and discrete descriptions. The numerical results are visually represented to demonstrate the impacts of MDD three temperatures and anisotropy on the ultrasound stress waves in FGA smart materials. The numerical findings verify the proposed methodology's validity and accuracy. We may conclude that the offered results are useful for comprehending the FGA smart materials. As a result, our findings contribute to the advancement of the industrial applications of FGA smart materials.

Keywords: boundary element method, modeling and simulation, three-temperature, memory-dependent derivative, laser ultrasonics, nonlinear thermal stress waves, functionally graded anisotropic, smart materials

1. Introduction

The development of smart structures in coming years is likely to be the most important task in a variety of scientific and technological fields such as bioengineering, informatics, aerospace engineering, microelectronics, medical treatment, energy, safety engineering, transportation, life science, and military technologies. As a result, various applications and industries are being created to support the growing importance of smart materials research (Fahmy et al., 2021).

The classical thermo-elasticity (CTE) theory of Duhamel (1837) and Neumann (1885), has two shortcomings: First, there are no elastic terms in the heat equation and secondly the heat equation predicts unlimited heat wave velocity. Biot (1956) developed the classical coupled thermo-elasticity (CCTE) theory to combat the primary shortcomings of CTE. However, both theories share the second shortcoming. As a result, many generalizations of Fourier's heat law have been developed to predict finite speeds of heat waves, such as the extended thermo-elasticity (ETE) theory of Lord and Shulman (L-S) (1967), temperature-rate-dependent thermo-elasticity (TRDTE) theory Green and Lindsay (G-L) (1972), three linear generalized thermoelasticity models of Green and Naghdi (G-N) (1992, 1993), low-temperature thermo-elasticity model of Hetnarski and Ignaczak (H-I) (1996), dual phase-lag thermoelasticity (DPLTE) theory of

* Author's e-mails: maselim@uqu.edu.sa, mohamed_fahmy@ci.suez.edu.eg
ORCID ID: 0000-0002-2417-3913

Tzou (1997) and Chandrasekharaiah (1998), Youssef (2006) two-temperature generalized thermoelasticity theory, three-phase-lag thermoelasticity (TPLTE) theory of Roy Choudhuri (2007), and three-temperature generalized thermoelasticity of Fahmy (2019).

Recently, the field of fractional calculus has attracted the interest of researchers in various areas including heat conduction, biophysics, control theory, fluid mechanics, electrochemistry, electrical engineering, bioengineering, viscoelasticity, viscoplasticity, biology, solid mechanics, signal and image processing, control theory and finance.

In 1819 Lacroix suggested the n-th derivative for the function $y = x^m$ as:

$$\frac{d^n}{dx^n} = \frac{\Gamma(m+1)}{\Gamma(m-n+1)} x^{m-n} \tag{1}$$

Liouville supposed that $\frac{d^v}{dx^v}(e^{ax}) = a^v e^{ax}$ for $v > 0$ to obtain:

$$\frac{d^v x^{-a}}{dx^v} = (-1)^v \frac{\Gamma(a+v)}{\Gamma(a)} x^{-a-v} \tag{2}$$

Laurent suggested the integration of arbitrary order $v > 0$ as follows:

$$ {}_cD_x^v f(x) = {}_cD_x^{m-\rho} f(x) = \frac{d^m}{dx^m}\left[\frac{1}{\Gamma(\rho)}\int_c^x (x-t)^{\rho-1} f(t)dt\right], \quad 0<\rho\le 1 \tag{3}$$

Cauchy introduced the following fractional-order derivative:

$$f_+^{(\alpha)} = \int f(\tau)\frac{(t-\tau)^{-\alpha-1}}{\Gamma(-\alpha)}d\tau \tag{4}$$

In 1967, Caputo suggested the following fractional derivative:

$$D_*^\alpha f(t) = \frac{1}{\Gamma(m-\alpha)}\int_0^t \frac{f^{(m)}(\tau)}{(t-\tau)^{\alpha+1-m}}d\tau \qquad m-1<\alpha<m,\ \alpha>0 \tag{5}$$

Diettelm (1997) introduced the following Caputo derivative:

$$D_a^\zeta f(\tau) = \int_a^\tau K_\zeta(\tau-\xi) f^{(m)}(\xi)d\xi \tag{6}$$

where:

$$K_\zeta(\tau-\xi) = \frac{(\tau-\xi)^{m-\zeta-1}}{\Gamma(m-\zeta)}, m-1<\zeta\le m \tag{7}$$

Wang and Li (2011) suggested the following MDD:

$$D_\omega^\zeta f(\tau) = \frac{1}{\omega}\int_{\tau-\omega}^{\tau} K_\zeta(\tau-\xi) f^{(m)}(\xi)d\xi \tag{8}$$

On the basis of Fahmy (2021a), we can write:

$$D_\omega f(\tau) = \frac{1}{\omega}\int_{\tau-\omega}^{\tau} K(\tau-\xi) f'(\xi)d\xi, \tag{9}$$

$$\omega > 0,\ 0 \le K(\tau-\xi) \le 1 \text{ for } \xi \in [\tau-\xi, \tau]$$

Now, we consider the following special case ($K(\tau - \xi) \equiv 1$):

$$D_\omega f(\tau) = \frac{1}{\omega}\int_{\tau-\omega}^{\tau} f'(\xi)d\xi = \frac{f(\tau)-f(\tau-\omega)}{\omega} \to f'(\tau) \tag{10}$$

where:

$$D_\omega f(\tau) \le \left|\frac{\partial f}{\partial \tau}\right| = \lim_{\omega\to 0}\frac{f(\tau+\omega)-f(\tau)}{\omega} \tag{11}$$

In the present paper, the boundary element method (Banerjee & Butterfield, 1981; Fahmy, 2011, 2012a, 2012b, 2013, 2018, 2021b, 2021c, 2021d, 2021e; Wrobel & Brebbia, 1987) has been implemented successfully for solving three-temperature memory dependent derivative (MDD) problems of ultrasound stress waves in functionally graded anisotropic (FGA) smart materials. The numerical results are depicted graphically to show the influences of the three temperatures and anisotropy on the nonlinear thermal stress components. The validity, efficiency, and accuracy of our proposed BEM technique were confirmed by comparing our BEM obtained results with the corresponding finite element method (FEM) results.

2. Formulation of the problem

The geometry of the considered problem is shown in Figure 1 for a smart structure that occupies the region $R = \{0 < x < \underline{\beta}, 0 < y < \underline{\alpha}, 0 < z < \underline{\gamma}\}$ bounded by a closed surface S as shown in Figure 1, where S_i ($i = 1, 2, 3, 4$) such that $S_1 + S_2 = S_3 + S_4 = S$. The governing equations for the ultrasound stress waves in FGA smart materials with memory-dependent derivatives can be expressed as (Fahmy, 2020):

$$\sigma_{ij,j} + \tau_{ij,j} + \rho F_i = \rho \ddot{u}_i \tag{12}$$

$$D_{i,i} = 0 \tag{13}$$

where:

$$\sigma_{ij} = (x+1)^m [C_{ijkl} e \delta_{ij} - \beta_{ab}(T_\alpha - T_{\alpha 0} + \tau_1 T_\alpha)] \tag{14}$$

$$D_i = (x+1)^m [e_{ijk} \varepsilon_{jk} + \mathbb{f}_{ik} E_k] \varepsilon_{ij} = \frac{1}{2}(u_{i,j} + u_{j,i}) \tag{15}$$

where: σ_{ij} – force stress tensor; D_i – electric displacement; F_i – mass force vector; ε_{ij} – strain tensor; ε_{ijk} – alternate tensor; u_i – displacement vector; ρ – constant elastic moduli; C_{ijkl} ($C_{ijkl} = C_{klij} = C_{jikl}$) – density; e_{ijk} – piezoelectric tensor; e – dilatation; $\mathbb{f}_{ik}$ – permittivity tensor; E_k – electric field vector; β_{ij} ($\beta_{ij} = \beta_{ji}$) – stress–temperature coefficients.

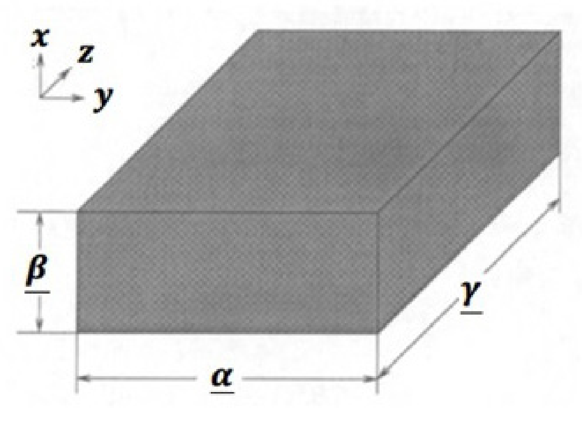

Fig. 1. Geometry of the considered problem

According to Fahmy (2019), the three-temperature heat conduction equations are:

$$c_e \frac{\partial T_e(r,\tau)}{\partial \tau} - \frac{1}{\rho} \nabla[\mathbb{K}_e \nabla T_e(r,\tau)] = -\mathbb{W}_{ei}(T_e - T_i) - \mathbb{W}_{ep}(T_e - T_p) \tag{16}$$

$$c_e \frac{\partial T_i(r,\tau)}{\partial \tau} - \frac{1}{\rho} \nabla[\mathbb{K}_i \nabla T_i(r,\tau)] = -\mathbb{W}_{ei}(T_e - T_i) \tag{17}$$

$$c_p T_p^3 \frac{\partial T_p(r,\tau)}{\partial \tau} - \frac{1}{\rho} \nabla[\mathbb{K}_p \nabla T_p(r,\tau)] = -\mathbb{W}_{ep}(T_e - T_p) \tag{18}$$

where: e, i, p – electron, ion, and phonon; (c_e, c_i, c_p) – specific heat capacities; ($\mathbb{K}_e$, $\mathbb{K}_i$, $\mathbb{K}_p$) – conductive coefficients; $\mathbb{W}_{ei}$ – electron-ion coefficient; $\mathbb{W}_{ep}$ – electron-phonon coefficient; (T_e, T_i, T_p) – temperature functions where: $\tau_{ij,j} = \mu_0^i \epsilon_{ijf} J_j H_f$ – i-component of the Lorentz force; $J(\tau) = (J_0\tau/\tau_3^2)e^{-\tau/\tau_3}$ – temporal profile of non-Gaussian laser pulse; $Q(x,\tau) = [(1-R)/x_0]e^{(-x_a/x_0)J(\tau)}$ – total energy intensity.

3. BEM solution of temperature field

On the basis of Fahmy (2019), equations (16)–(18) can be expressed as:

$$\nabla[(\delta_{1j}\mathbb{K}_\alpha + \delta_{2j}\mathbb{K}_\alpha^*)\nabla T_\alpha(r,\tau)] - \overline{\mathbb{W}}(r,\tau) = c_\alpha \rho \delta_1 \delta_{1j} D_{\omega_\alpha} T_\alpha(r,\tau) \tag{19}$$

which can be written as:

$$L_{ab} T_\alpha(r,\tau) = f_{ab} \tag{20}$$

in which:

$$L_{ab} = \nabla[(\delta_{1j}\mathbb{K}_\alpha + \delta_{2j}\mathbb{K}_\alpha^*)\,\nabla] \tag{21}$$

$$f_{ab} = \overline{\overline{\mathbb{W}}}(r,\tau) + \overline{\mathbb{W}}(r,\tau) \tag{22}$$

where:

$$\overline{\mathbb{W}}(r,\tau) = \begin{cases} \rho\mathbb{W}_{ei}(T_e - T_i) + \rho\mathbb{W}_{er}(T_e - T_p) + \overline{\overline{\mathbb{W}}} & \alpha = e,\ \delta_1 = 1 \\ -\rho\mathbb{W}_{ei}(T_e - T_i) + \overline{\overline{\mathbb{W}}} & \alpha = 1,\ \delta_1 = 1 \\ -\rho\mathbb{W}_{er}(T_e - T_p) + \overline{\overline{\mathbb{W}}} & \alpha = p,\ \delta_1 = T_p^3 \end{cases} \tag{23}$$

$$\overline{\overline{\mathbb{W}}}(r,\tau) = F(r,\tau) - \frac{\delta_{2k} \quad \alpha}{\omega_\alpha} \int_{\tau-\omega_\alpha}^{\tau} K(\tau-\xi) \frac{\partial}{\partial \xi}(\nabla^2 T_\alpha(r,\tau))d\xi + \frac{\rho c_\alpha \delta_1 \delta_{1j}}{\omega_\alpha} \int_{\tau-\omega_\alpha}^{\tau} K(\tau-\xi) \frac{\partial}{\partial \xi}(T_\alpha(r,\tau))d\xi + \frac{\rho c_\alpha(\tau_0 + \delta_{1j}\tau_2 + \delta_{2j})}{\omega_\alpha} \int_{\tau-\omega_\alpha}^{\tau} K(\tau-\xi) \frac{\partial^2}{\partial \xi^2}(T_\alpha(r,\tau))d\xi \tag{24}$$

$$F(r,\tau) = \beta_{ab} T_{\alpha 0}[\text{Å}\delta_{1j}\dot{u}_{a,b} + (\tau_0 + \delta_{2j})\ddot{u}_{a,b}] \tag{25}$$

where: Å – unified parameter which introduced to consolidate all theories into a unified equations system, u_a – displacement vector.

and:

$$\mathbb{W}_{ei} = \rho \mathbb{A}_{ei} T_e^{-\frac{2}{3}}, \quad \mathbb{W}_{er} = \rho \mathbb{A}_{er} T_e^{-\frac{1}{2}}$$
$$\mathbb{K}_\alpha = \mathbb{A}_\alpha T_\alpha^{\frac{5}{2}}, \ \alpha = e, i, \ \mathbb{K}_p = \mathbb{A}_p T_p^{3+} \tag{26}$$

where ω_α(> 0) ($\alpha = e$, i, and p) are the delay times.

The total energy is:

$$P = P_e + P_i + P_p,\ P_e = c_e T_e,\ P_i = c_i T_i,\ P_p = \frac{1}{4} c_p T_p^4 \tag{27}$$

Now, we consider the following initial and boundary conditions:

$$T_\alpha(x,y,0) = T_\alpha^0(x,y) = g_1(x,\tau) \tag{28}$$

$$\mathbb{K}_\alpha \frac{\partial T_\alpha}{\partial n}\bigg|_{\Gamma_1} = 0, \quad \alpha = e, i, T_p\Big|_{\Gamma_1} = g_2(x,\tau) \tag{29}$$

$$\mathbb{K}_\alpha \frac{\partial T_\alpha}{\partial n}\bigg|_{\Gamma_2} = 0, \quad \alpha = e, i, p \tag{30}$$

Now, we assume that the fundamental solutions T^*_α satisfies:

$$L_{ab}T^*_\alpha = f_{ab} \qquad (31)$$

By applying the procedure of Fahmy (2019) to (19), we get:

$$CT_\alpha = \frac{D}{\mathbb{K}_\alpha}\int_0^\tau\int_S [T_\alpha q^* - T^*_\alpha q]dSd\tau + \frac{D}{\mathbb{K}_\alpha}\int_0^\tau\int_R bT^*_\alpha qdRd\tau + \int_R T^i_\alpha T^*_\alpha\Big|_{\tau=0} dR \qquad (32)$$

which can be written as:

$$CT_\alpha = \int_S [T_\alpha q^* - T^*_\alpha q]dS - \int_R \frac{\mathbb{K}_\alpha}{D}\frac{\partial T^*_\alpha}{\partial\tau}T_\alpha dR \qquad (33)$$

Now, we assume that:

$$\frac{\partial T^*_\alpha}{\partial\tau} \cong \sum_{j=1}^{N} f^j(r)^j a^j(\tau) \qquad (34)$$

and:

$$\nabla^2\hat{T}^j_\alpha = f^j \qquad (35)$$

where: $f^j(r)$ – known functions; $a^j(\tau)$ – unknown coefficients.

Then, from (33) we obtain the following boundary integral equation:

$$CT_\alpha = \int_S [T_\alpha q^* - T^*_\alpha q]dS + \sum_{j=1}^{N} a^j(\tau)D^{-1}\left(C\hat{T}^j_\alpha - \int_S [T^j_\alpha q^* - \hat{q}^j T^*_\alpha]dS\right) \qquad (36)$$

where:

$$\hat{q}^j = -\mathbb{K}_\alpha\frac{\partial\hat{T}^j_\alpha}{\partial n} \qquad (37)$$

and:

$$a^j(\tau) = \sum_{i=1}^{N} f^{-1}_{ji}\frac{\partial T_\alpha(r_i,\tau)}{\partial\tau} \qquad (38)$$

where f^{-1}_{ji} are the coefficients of F^{-1} as defined in Wrobel and Brebbia (1987) as:

$$\{F\}_{ji} = f^j(r_i) \qquad (39)$$

By discretizing (36) and using (38), we obtain (Fahmy, 2019):

$$C\dot{T}_\alpha + HT_\alpha = GQ \qquad (40)$$

where:

$$C = -[H\hat{T}_\alpha - G\hat{Q}]F^{-1}D^{-1} \qquad (41)$$

in which:

$$\{\hat{T}\}_{ij} = \hat{T}_j(x_i) \qquad (42)$$

$$\{\hat{Q}\}_{ij} = \hat{q}_j(x_i) \qquad (43)$$

To solve Equation (41), we interpolate T_α and q as:

$$T_\alpha = (1-\theta)T^m_\alpha + \theta T^{m+1}_\alpha \qquad (44)$$

$$q = (1-\theta)q^m + \theta q^{m+1} \qquad (45)$$

where $0 \le \theta = (\tau - \tau^m)/(\tau^{m+1} - \tau^m) \le 1$.

By time differentiation of Equation (44) we obtain:

$$\dot{T}_\alpha = \frac{dT_\alpha}{d\theta}\frac{d\theta}{d\tau} = \frac{T^{m+1}_\alpha - T^m_\alpha}{\tau^{m+1}-\tau^m} = \frac{T^{m+1}_\alpha - T^m_\alpha}{\Delta\tau^m} \qquad (46)$$

By substitution from (44)–(46) into (40), we get:

$$\left(\frac{C}{\Delta\tau^m} + \theta H\right)T^{m+1}_\alpha - \theta GQ^{m+1} = \left(\frac{C}{\Delta\tau^m} - (1-\theta)H\right)T^m_\alpha + (1-\theta)GQ^m \qquad (47)$$

Hence, we obtain:

$$\mathbb{a}X = \mathbb{b} \qquad (48)$$

4. BEM solution of the displacement field

On the basis of the weighted residual method, equations (12) and (13) in terms of the weighting functions u^*_i and Φ^*_i can be written as follows:

$$\int_R (\sigma_{ij,j} + U_i)u^*_i dR = 0 \qquad (49)$$

$$\int_R (D_{,i})\Phi^*_i dR = 0 \qquad (50)$$

in which:

$$U_i = \tau_{ij,j} + \rho F_i - \rho\ddot{u}_i, \qquad (51)$$

$$u_i = \overline{u}_i \quad \text{on } S_1 \qquad (52)$$

$$\lambda_i = \sigma_{ij}n_j = \overline{\lambda}_i \quad \text{on } S_2 \qquad (53)$$

$$\Phi = \overline{\Phi} \quad \text{on } S_3 \qquad (54)$$

$$Q = \frac{\partial\Phi}{\partial n} = \overline{Q} \quad \text{on } S_4 \qquad (55)$$

By integrating the first term of (49) and (50) by parts, we have:

$$-\int_R \sigma_{ij} u^*_{i,j} dR + \int_R U_i u^*_i dR = -\int_{S_2} \lambda_i u^*_i dS \tag{56}$$

$$-\int_R D\Phi^*_{i,i} dR = -\int_{S_4} Q_i \Phi^*_i dS \tag{57}$$

According to Huang and Liang (1996), the integral equation may be written as:

$$\begin{aligned}&-\int_R \sigma_{ij,j} u^*_i dR + +\int_R U_i u^*_i dR - \int_R D\Phi^*_{i,i} dR = \\ &\int_{S_2} (\lambda_i - \bar{\lambda}_i) u^*_i dS + \int_{S_1} (\bar{u}_i - u_i)\lambda^*_i dS + \\ &\int_{S_4} (Q_i - \bar{Q}_i)\Phi^*_i dS + \int_{S_3} (\bar{\Phi}_i - \Phi_i) Q^*_i dS\end{aligned} \tag{58}$$

which can be written as:

$$\begin{aligned}&-\int_R \sigma_{ij}\varepsilon^*_{ij} dR + \int_R U_i u^*_i dR - \int_R D\Phi^*_{i,i} dR = \\ &-\int_{S_2} \bar{\lambda}_i u^*_i dS - \int_{S_1} \lambda_i u^*_i dS + \int_{S_1} (\bar{u}_i - u_i)\lambda^*_i dS - \\ &\int_{S_4} \bar{Q}_i \Phi^*_i dS - \int_{S_3} Q_i \Phi^*_i dS + \int_{S_3} (\bar{\Phi}_i - \Phi_i) Q^*_i dS\end{aligned} \tag{59}$$

On the basis of Erigen (1968), the elastic stress may be written as:

$$\sigma_{ij} = \mathbb{A}_{ijkl}\varepsilon_{kl}, \tag{60}$$

where:

$$\mathbb{A}_{ijkl} = \mathbb{A}_{klij} \tag{61}$$

Hence, Equation (59) can be rewritten as:

$$\begin{aligned}&-\int_R \sigma^*_{ij}\varepsilon_{ij} dR + \int_R U_i u^*_i dR - \int_R D\Phi^*_{i,i} dR = \\ &-\int_{S_2} \bar{\lambda}_i u^*_i dS - \int_{S_1} \lambda_i u^*_i dS + \int_{S_1} (\bar{u}_i - u_i)\lambda^*_i dS - \\ &\int_{S_4} \bar{Q}_i \Phi^*_i dS - \int_{S_3} Q_i \Phi^*_i dS + \int_{S_3} (\bar{\Phi}_i - \Phi_i) Q^*_i dS\end{aligned} \tag{62}$$

Integration by parts again, yields:

$$\begin{aligned}&\int_R \sigma^*_{ij,j} u_i dR = \\ &-\int_S u^*_i \lambda_i dS - \int_S \Phi^*_i Q_i dS + \int_S \lambda^*_i u_i dS + \int_S Q^*_i \Phi_i dS\end{aligned} \tag{63}$$

The weighting functions of $U_i = \Delta^n$ can be expressed as:

$$\sigma^*_{lj,j} + \Delta^n e_l = 0 \tag{64}$$

According to Dragoş (1984), we get:

$$u^*_i = u^*_{li} e_l,\ \Phi^*_i = \Phi^*_{li} e_l,\ \lambda^*_i = \lambda^*_{li} e_l,\ Q^*_i = Q^*_{li} e_l \tag{65}$$

The weighting functions of $U_i = 0$ and $V_i = \Delta^n$ along e_l are:

$$\sigma^{**}_{lj,j} = 0 \tag{66}$$

On the basis of Dragoş (1984), we get:

$$u^*_i = u^{**}_{li} e_l,\ \Phi^*_i = \Phi^{**}_{li} e_l,\ \lambda^*_i = \lambda^{**}_{li} e_l,\ Q^*_i = Q^{**}_{li} e_l \tag{67}$$

By employing (65) and (67) in (63) we have:

$$C^n_{li} u^n_i = -\int_S \lambda^*_{li} u_i dS - \int_S Q^*_{li} \Phi_i dS + \int_S u^*_{li} \lambda_i dS + \int_S \Phi^*_{li} Q_i dS \tag{68}$$

$$C^n_{li} \omega^n_i = -\int_S \lambda^{**}_{li} u_i dS - \int_S Q^{**}_{li} \Phi_i dS + \int_S u^{**}_{li} \lambda_i dS + \int_S \Phi^{**}_{li} Q_i dS \tag{69}$$

Thus, we obtain (see Fahmy et al., 2021):

$$\begin{aligned}&C^n q^n = -\int_S \mathbb{p}^* \mathbb{q} dS + \int_S \mathbb{q}^* \mathbb{p} dS + \int_S \mathbb{d}^* \Phi dS + \\ &\int_S \mathbb{f}^* \frac{\partial \Phi}{\partial n} dS\end{aligned} \tag{70}$$

where:

$$\mathrm{C^n} = \begin{bmatrix} \mathrm{C}_{11} & \mathrm{C}_{12} & \\ \mathrm{C}_{21} & \mathrm{C}_{22} & \\ & & \end{bmatrix},\ \mathbb{q}^* = \begin{bmatrix} \mathrm{u}^*_{11} & \mathrm{u}^*_{12} & 0 \\ \mathrm{u}^*_{21} & \mathrm{u}^*_{22} & 0 \\ \mathrm{u}^*_{31} & \mathrm{u}^*_{32} & 0 \end{bmatrix}$$

$$\mathbb{p}^* = \begin{bmatrix} \lambda^{**}_{11} & \lambda^{**}_{12} & 0 \\ \lambda^{**}_{21} & \lambda^{**}_{22} & 0 \\ \lambda^{**}_{31} & \lambda^{**}_{32} & 0 \end{bmatrix},\ \mathbb{q} = \begin{bmatrix} \mathrm{u}_1 \\ \mathrm{u}_2 \\ \omega_3 \end{bmatrix},\ \mathbb{p} = \begin{bmatrix} \lambda_1 \\ \lambda_2 \\ \mu_3 \end{bmatrix} \tag{71}$$

$$\mathbb{d}^* = \begin{bmatrix} \mathbb{d}^*_1 \\ \mathbb{d}^*_2 \\ 0 \end{bmatrix},\ \mathbb{f}^* = \begin{bmatrix} \mathbb{f}^*_1 \\ \mathbb{f}^*_2 \\ 0 \end{bmatrix}$$

Now, we assume that:

$$\mathbb{q} = \psi \mathbb{q}^j,\ \mathbb{p} = \psi \mathbb{p}^j,\ \Phi = \psi_0 \Phi^j,\ \frac{\partial \Phi}{\partial n} = \psi_0 \left(\frac{\partial \Phi}{\partial n}\right)^j \tag{72}$$

Therefore, we can write (70) as:

$$\begin{aligned}&C^n \mathbb{q}^n = \sum_{j=1}^{N_e} \left[-\int_{\Gamma_j} \mathbb{p}^* \psi d\Gamma \right] \mathbb{q}^j + \sum_{j=1}^{N_e} \left[\int_{\Gamma_j} \mathbb{q}^* \psi d\Gamma \right] \mathbb{p}^j + \\ &\sum_{j=1}^{N_e} \left[\int_{\Gamma_j} \mathbb{d}^* \psi_0 d\Gamma \right] \Phi^j + \sum_{j=1}^{N_e} \left[\int_{\Gamma_j} \mathbb{f}^* \psi_0 d\Gamma \right] \left(\frac{\partial \Phi}{\partial n}\right)^j\end{aligned} \tag{73}$$

Equation after integration can be written as:

$$C^i \mathbb{q}^i = -\sum_{j=1}^{N_e} \hat{\mathbb{H}}^{ij} \mathbb{q}^j + \sum_{j=1}^{N_e} \hat{\mathbb{G}}^{ij} \mathbb{p}^j + \sum_{j=1}^{N_e} \hat{\mathbb{D}}^{ij} \Phi^j + \sum_{j=1}^{N_e} \hat{\mathbb{F}}^{ij} \left(\frac{\partial \Phi}{\partial n} \right)^j \quad (74)$$

By using the following representation:

$$\mathbb{H}^{ij} = \begin{cases} \hat{\mathbb{H}}^{ij} & \text{if} \quad i \neq j \\ \hat{\mathbb{H}}^{ij} + C^i & \text{if} \quad i = j \end{cases} \quad (75)$$

Thus, we can write (74) as follows:

$$\sum_{j=1}^{N_e} \mathbb{H}^{ij} \mathbb{q}^j = \sum_{j=1}^{N_e} \hat{\mathbb{G}}^{ij} \mathbb{p}^j + \sum_{j=1}^{N_e} \hat{\mathbb{D}}^{ij} \Phi^j + \sum_{j=1}^{N_e} \hat{\mathbb{F}}^{ij} \left(\frac{\partial \Phi}{\partial n} \right)^j \quad (76)$$

The global matrix equation for all i nodes can be expressed as:

$$\mathbb{H}\mathbb{Q} = \mathbb{G}\mathbb{P} + \mathbb{D}\Theta + \mathbb{F}\mathbb{S} \quad (77)$$

where: $\mathbb{Q}$ – displacements; $\mathbb{P}$ – tractions; Θ – electric potential; $\mathbb{S}$ – electric potential gradient vector.

Which can be written in the following form:

$$\mathbb{A}\mathbb{X} = \mathbb{B} \quad (78)$$

For solving the resulting linear algebraic system of equations, an explicit staggered algorithm of Fahmy (2019) based on the communication-avoiding Arnoldi (CA-Arnoldi) preconditioner is developed as follows:

Step. 1. We obtain the temperature field in terms of the displacement field from (48).

Step. 2. We forecast the displacement field and, as a result, the temperature field.

Step. 3. From (78), we correct the displacement field using the calculated temperature.

5. Numerical results and discussions

The proposed methodology in this work, if implemented, should be applicable to a wide range of three-temperature smart structures problems. There are no available literature for comparison due to the nature of the problems under consideration. As a result, some literature can be thought of as special examples of our BEM results. The results of the special example under examination are presented in Figures 3–6 to show the impacts of MDD three temperatures and anisotropy on the nonlinear thermal stress waves in FGA smart structures.

The boundary of the considered BEM model has been discretized into 42 linear boundary elements and 68 internal points, as shown in Figure 2. Also, the domain of the considered FEM model has been discretized into 1896 second-order quadrilateral elements and 5986 nodes.

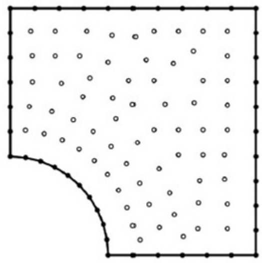

Fig. 2. Boundary element model of the considered problem

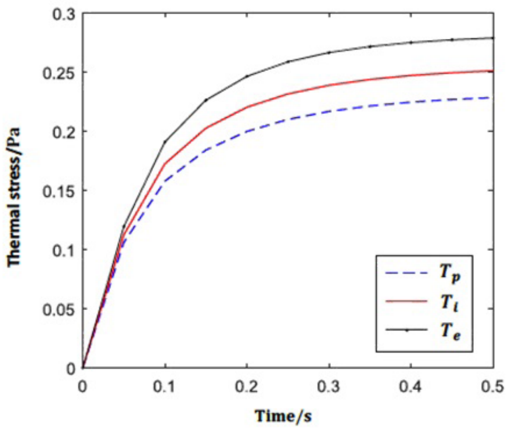

Fig. 3. Variation of the thermal stress waves with time τ for T_e, T_i and T_p (isotropic material)

Figure 3 shows the variation of the thermal stress waves with time τ for T_e, T_i and T_p in an isotropic material. It can be seen from this figure that the three temperatures have a significant effect on the thermal stress waves of functionally graded isotropic smart materials.

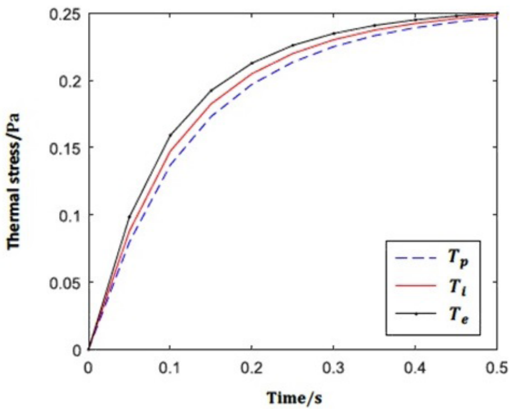

Fig. 4. Variation of the thermal stress waves with time τ for T_e, T_i and T_p (orthotropic material)

Figure 4 illustrates the variation of the thermal stress waves with time τ for T_e, T_i and T_p in an orthotropic material. The three temperatures have a considerable effect on the thermal stress waves of functionally graded orthotropic smart materials, as seen in this figure.

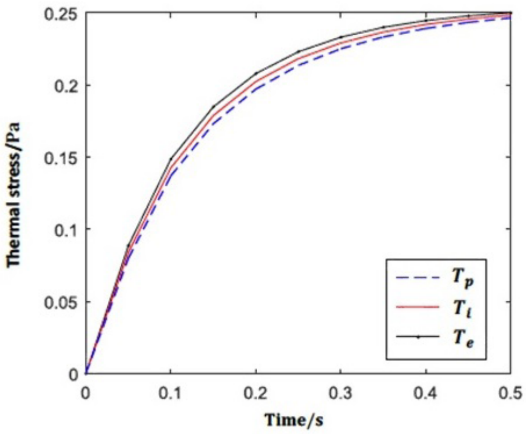

Fig. 5. Variation of the thermal stress waves with time τ for T_e, T_i and T_p (anisotropic material)

Figure 5 illustrates the variation of the thermal stress waves with time τ for T_e, T_i and T_p in an anisotropic material. The three temperatures have a considerable effect on the thermal stress waves of functionally graded anisotropic smart materials, as seen in this figure.

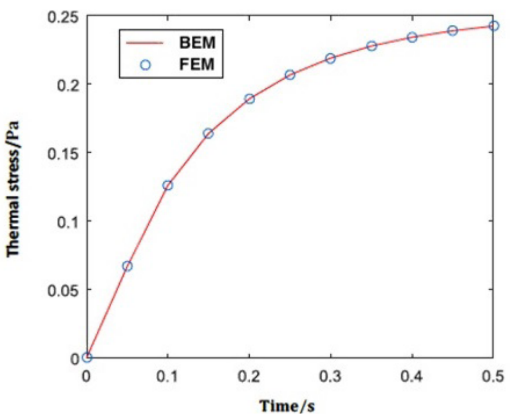

Fig. 6. Variation of the thermal stress waves with time τ for boundary and finite element methods

The validity and correctness of our suggested model have been confirmed by comparing the one-dimensional BEM results graphically with those produced using the finite element method (FEM) of Shakeriaski and Ghodrat (2020). These results show that the BEM results are in excellent agreement with the FEM results.

The domain methods include the solution of the entire domain, including the boundary domain of the problems of the current theory, yet the proposed BEM only needs to solve the boundary unknowns. As a result, BEM can be used to solve such problems efficiently than domain methods. Based on the performed research, it is possible to conclude that the proposed BEM technique is efficient and stable for problems of the current theory. BEM users only need to deal with real geometry boundaries when dealing with closed or open boundary problems. The problems of the current theory are open boundary problems. FDM and FEM employ artificial boundaries that are far from the true structure to solve these open boundary problems. These artificial boundaries also pose a significant difficulty for FDM and FEM users.

6. Conclusion

The goal of this study is to present a novel theory known as three-temperature memory-dependent derivative (MDD) of ultrasound stress waves in functionally graded anisotropic (FGA) Smart Materials. Because of the nonlinear anisotropic mechanical properties of the investigated smart materials, it is extremely difficult to address the difficulties of this theory. As a result, we suggest a novel boundary element model for dealing with such problems. The suggested BEM technique incorporates the benefits of both continuous and discrete descriptions because the CA kernels of s-step Krylov techniques are faster than the kernels of ordinary Krylov techniques. As a result, to solve the linear systems emerging from the BEM discretization, we developed an explicit staggered approach based on the CA-Arnoldi technique. The numerical findings are graphed to show the impact of MDD three temperatures and anisotropy on the laser-generated waves in FGA smart structures. The numerical results further indicate the suggested technique's validity, precision, and efficiency. The effective methodology provided here can be used to solve a wide range of FGA smart materials problems.

References

Banerjee, P.K., & Butterfield, R. (1981). *Boundary element methods in engineering science*. McGraw-Hill.
Biot, M.A. (1956). Thermoelasticity and irreversible thermo-dynamics. *Journal of Applied Physics*, *27*(3), 249–253. https://doi.org/10.1063/1.1722351.

Chandrasekharaiah, D.S. (1998). Hyperbolic thermoelasticity: a review of recent literature. *Applied Mechanics Reviews*, *51*(12), 705–729. https://doi.org/10.1115/1.3098984.

Diettelm, K. (1997). Generalized compound quadrature formulae for finite-part integrals. *IMA Journal of Numerical Analysis*, *17*(3), 479–493. https://doi.org/10.1093/imanum/17.3.479.

Dragoş, L. (1984). Fundamental solutions in micropolar elasticity. *International Journal of Engineering Science*, *22*(3), 265–275. https://doi.org/10.1016/0020-7225(84)90007-7.

Duhamel, J. (1837). Some memoire sur les phenomenes thermo-mechanique. *Journal de l'École Polytechnique*, *15*, 1–57.

Erigen, A.C. (1968). Theory of micropolar elasticity, In H. Liebowitz (Ed.). *Fracture. An advanced treatise* (vol. 2: *Mathematical fundamentals*). Academic Press.

Fahmy, M.A. (2011). A time-stepping DRBEM for magneto-thermo-viscoelastic interactions in a rotating nonhomogeneous anisotropic solid. *International Journal of Applied Mechanics*, *3*(4), 711–734. https://doi.org/10.1142/S1758825111001202.

Fahmy, M.A. (2012a). A time-stepping DRBEM for the transient magneto-thermo-visco-elastic stresses in a rotating non-homogeneous anisotropic solid. *Engineering Analysis with Boundary Elements*, *36*(3), 335–345. https://doi.org/10.1016/j.enganabound.2011.09.004.

Fahmy, M.A. (2012b). Transient magneto-thermoviscoelastic plane waves in a non-homogeneous anisotropic thick strip subjected to a moving heat source. *Applied Mathematical Modelling*, *36*(10), 4565–4578. https://doi.org/10.1016/j.apm.2011.11.036.

Fahmy, M.A. (2013). Implicit–Explicit time integration DRBEM for generalized magneto-thermoelasticity problems of rotating anisotropic viscoelastic functionally graded solids. *Engineering Analysis with Boundary Elements*, *37*(1), 107–115. https://doi.org/10.1016/j.enganabound.2012.08.002.

Fahmy, M.A. (2018). Boundary element algorithm for modeling and simulation of dual-phase lag bioheat transfer and biomechanics of anisotropic soft tissues. *International Journal of Applied Mechanics*, *10*(10), 1850108. https://doi.org/10.1142/S1758825118501089.

Fahmy, M.A. (2019). A New Boundary Element Strategy for Modeling and Simulation of Three Temperatures Nonlinear Generalized Micropolar-Magneto-Thermoelastic Wave Propagation Problems in FGA Structures. *Engineering Analysis with Boundary Elements*, *108*, 192–200. https://doi.org/10.1016/j.enganabound.2019.08.006.

Fahmy, M.A. (2020). Boundary element algorithm for nonlinear modeling and simulation of three temperature anisotropic generalized micropolar piezothermoelasticity with memory-dependent derivative. *International Journal of Applied Mechanics*, *12*(3), 2050027. https://doi.org/10.1142/S1758825120500271.

Fahmy, M.A. (2021a). A novel BEM for modeling and simulation of 3T nonlinear generalized anisotropic micropolar-thermoelasticity theory with memory dependent derivative. *CMES – Computer Modeling in Engineering & Sciences*, *126*(1), 175–199. https://doi.org/10.32604/cmes.2021.012218.

Fahmy, M.A. (2021b). A new boundary element algorithm for a general solution of nonlinear space-time fractional dual-phase-lag bio-heat transfer problems during electromagnetic radiation. *Case Studies in Thermal Engineering*, *25*, 100918. https://doi.org/10.1016/j.csite.2021.100918.

Fahmy, M.A. (2021c). A new boundary element formulation for modeling and simulation of three-temperature distributions in carbon nanotube fiber reinforced composites with inclusions. *Mathematical Methods in the Applied Science*. https://doi.org/10.1002/mma.7312 [in progress].

Fahmy, M.A. (2021d). A new boundary element algorithm for modeling and simulation of nonlinear thermal stresses in micropolar FGA composites with temperature-dependent properties. *Advanced Modeling and Simulation in Engineering Sciences*, *8*, 1–23. https://doi.org/10.1186/s40323-021-00193-6.

Fahmy, M.A. (2021e). A New BEM for Fractional Nonlinear Generalized Porothermoelastic Wave Propagation Problems. *Computers, Materials and Continua*, *68*(1), 59–76. https://doi.org/10.32604/cmc.2021.015115.

Fahmy, M.A., Shaw, S., Mondal, S., Abouelregal, A.E., Lotfy, K., Kudinov, I.V., & Soliman, A.H. (2021). Boundary Element Modeling for Simulation and Optimization of Three-Temperature Anisotropic Micropolar Magneto-thermoviscoelastic Problems in Porous Smart Structures Using NURBS and Genetic Algorithm. *International Journal of Thermophysics*, *42*, 29. https://doi.org/10.1007/s10765-020-02777-7.

Green, A.E., & Lindsay, K.A. (1972). Thermoelasticity. *Journal of Elasticity*, *2*(1), 1–7. https://doi.org/10.1007/BF00045689.

Green, A.E., & Naghdi, P.M. (1992). On undamped heat waves in an elastic solid. *Journal of Thermal Stresses*, *15*(2), 253–264. https://doi.org/10.1080/01495739208946136.

Green, A.E., & Naghdi, P.M. (1993). Thermoelasticity without energy dissipation. *Journal of Elasticity*, *31*(3), 189–208. https://doi.org/10.1007/BF00044969.

Hetnarski, R.B., & Ignaczak, J. (1996). Soliton-like Waves in a Low-temperature Nonlinear Thermoelastic Solid. *International Journal of Engineering Science*, *34*(15), 1767–1787. https://doi.org/10.1016/S0020-7225(96)00046-8.

Huang, F.Y., & Liang, K.Z. (1996). Boundary element method for micropolar thermoelasticity. *Engineering Analysis with Boundary Elements*, *17*(1), 19–26. https://doi.org/10.1016/0955-7997(95)00086-0.

Lord, H.W., & Shulman, Y. (1967). A generalized dynamical theory of thermoelasticity. *Journal of the Mechanics and Physics of Solids*, *15*(5), 299–309. https://doi.org/10.1016/0022-5096(67)90024-5.

Neumann, F. (1885). *Vorlesungen über die Theorie der Elasticität*. Brestau.

Roy Choudhuri, S.K. (2007). On A Thermoelastic Three-Phase-Lag Model. *Journal of Thermal Stresses*, *30*(3), 231–238. https://doi.org/10.1080/01495730601130919.

Shakeriaski, F., & Ghodrat, M. (2020). The nonlinear response of Cattaneo-type thermal loading of a laser pulse on a medium using the generalized thermoelastic model. *Theoretical and Applied Mechanics Letters*, *10*(4), 286–297. https://doi.org/10.1016/j.taml.2020.01.030.

Tzou, D.Y. (1997). *Macro-to microscale heat transfer. The lagging behavior*. Taylor & Francis.

Wang, J.L., & Li, H.F. (2011). Surpassing the fractional derivative: Concept of the memory-dependent derivative. *Computers and Mathematics with Applications*, *62*(3), 1562–1567. https://doi.org/10.1016/j.camwa.2011.04.028.

Wrobel, L.C., & Brebbia, C.A. (1987). The Dual Reciprocity Boundary Element formulation for nonlinear diffusion problems. *Computer Methods in Applied Mechanics and Engineering*, *65*(2), 147–164. https://doi.org/10.1016/0045-7825(87)90010-7.

Youssef, H. (2006). Theory of two-temperature-generalized thermoelasticity. *IMA Journal of Applied Mathematics*, *71*(3), 383–390. https://doi.org/10.1093/imamat/hxh101.